COMPUTER AIDED ENGINEERING

Integrated simulation of the process chain composite extrusion–milling–welding for lightweight frame structures

**Michael F. Zaeh · A. Erman Tekkaya · Dirk Biermann ·
Andreas Zabel · Mirko Langhorst · Alexander Schober ·
Thomas Kloppenborg · Markus Steiner · Eduard Ungemach**

Abstract Generally, the manufacturing of lightweight frame structures involves various processes that yield the final product. Simulation methods can be used to optimise the different process steps. When chaining these process steps together in the simulation, software interfaces become necessary to realise an integrated virtual process chain. In this paper two approaches are presented that solve this issue and demonstrate it for an exemplary part. Different software tools with appropriate interfaces and the use of only one software tool for the simulation of the whole process chain are investigated respectively. The results of both approaches are analysed and relevant conclusions are deduced.

Keywords Simulation · Process chain · Lightweight frame structures · Software interfaces · Composite material

1 General introduction

The Transregional Collaborative Research Centre 10 (SFB/TR 10) "Integration of forming, cutting and joining for the flexible production of lightweight frame structures" is funded by the German Research Foundation (DFG) at the TU Dortmund, the Universitaet Karlsruhe and the Technische Universitaet Muenchen. A major objective is the investigation of the integrated process chain including the

processes of extrusion, cutting and joining in reality as well as in simulation. In the field of simulation the subprojects B1 (composite extrusion simulation), B2 (simulation of the five-axis milling process), B3 (mechanical simulation of the machining process), B4 (welding simulation) and C7 (simulation of the process chain) are researching the different manufacturing processes and their influences regarding the process chain. Within the TR 10 the use of simulation methods is on the one hand to gain knowledge of the applied processes and on the other hand to optimize them regarding particular variables. Thus, optimized process parameters can be computed to minimize structural workpiece reactions such as stresses und strains. In particular, these variables are of special interest because the investigated structures within the TR 10 are transportation related and thus, a high safety factor is demanded. Hence, information about critical stress situations in the structure is in the focus of interest.

A challenge for the real process chain is the machining of steel reinforced aluminium. This novel material is difficult to cut and join because of the different material properties of steel and aluminium.

Designing lightweight structures requires a detailed knowledge of the final part properties, especially the distortions and the residual stresses, which are a result of the entire manufacturing history. By using simulation methods it is possible to determine the structural effects of every single process step on the work piece and at last of the whole manufacturing chain. In contrast to reality, a challenge arises in the simulation when actually chaining the different manufacturing steps together. Due to the different data formats of the various software tools that are used in the subprojects interfaces between these systems are necessary to realise an integrated virtual process chain (Fig. 1).

In addition, an alternative method without using interfaces is also investigated in this paper. Namely, the entire

M. F. Zaeh · M. Langhorst (✉) · A. Schober
Technische Universität München, Munich, Germany
e-mail: mirko.langhorst@iwb.tum.de

A. E. Tekkaya · D. Biermann · A. Zabel · T. Kloppenborg ·
M. Steiner · E. Ungemach
TU Dortmund, Dortmund, Germany

Fig. 1 Interrelation of the subprojects involved in the virtual process chain
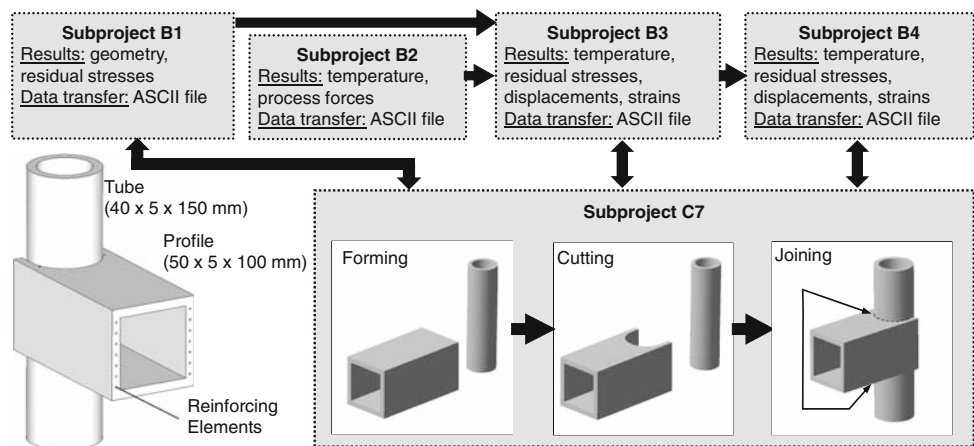
process chain is simulated within only one software environment hence eliminating the need of software interfaces. In doing so, a few simplifications concerning the different processes are necessary.

In this paper a T-joint (Fig. 1) of a non-reinforced tube and a reinforced square profile is examined. The entire process chain, which consists of the processes composite extrusion, milling and welding, is represented by this part.

The following chapters detail the different simulation approaches for the respective manufacturing processes. Additionally, information on the import and export of result data is given.

2 Simulation of the composite extrusion process (subproject B1)

2.1 Introduction

The process chain starts with the composite extrusion process. Here, a continuous reinforcement of aluminium profiles increases the mechanical properties, e.g. stiffness and strength, as well as the field of application [1]. A preheated billet of aluminium EN-AW 6060 is supplied in the extrusion press and then extruded through the die. For the process of composite extrusion special bridge dies are utilized to divide the aluminium base material into separate streams. The reinforcements are supplied in between the material flow at the moment the material rejoins under high temperature and high pressure in the welding chamber (Fig. 2). Generally, the composite profile leaves the die orifice at temperatures ranging from 450 to 550°C. Then a cooling operation starts that induces residual stresses in the composite profile. Micrographs at higher magnifications prove that the interface between the embedded wires and the surrounding matrix is free of gaps. The bonding area between the different materials was also

investigated. It could be shown that not only a form closure but also an adhesive bond occurs between the materials [2].

However, depending on the combination of the matrix and the reinforcement material residual stresses arise due to the different coefficients of thermal expansion [3]. For the design of structures, as well as for subsequent manufacturing steps, the residual stresses are of high importance, e.g. the yield strength can be increased in case of compressive residual stresses in the reinforcement material or deflections can occur in case of a subsequent milling or welding operation.

2.2 Simulation and results

For the computation of the residual stresses and the investigation of their influence on the subsequent manufacturing steps a three dimensional numerical model was set up. For simplification not the complete forming process was modelled but only the cooling process. Here, the profile temperature of 450°C was reduced in 100 time steps to ambient temperature (20°C). Sticking boundary conditions were used between the aluminium and the steel material according to the research results in [2]. Both materials were modelled as elastoplastic materials in the
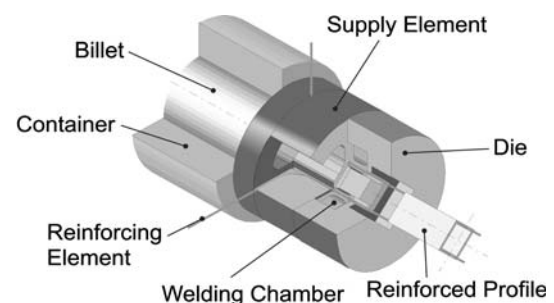
Fig. 2 Process principle of composite extrusion

Fig. 3 Results of the temperature field and the effective stress distribution after the cooling process
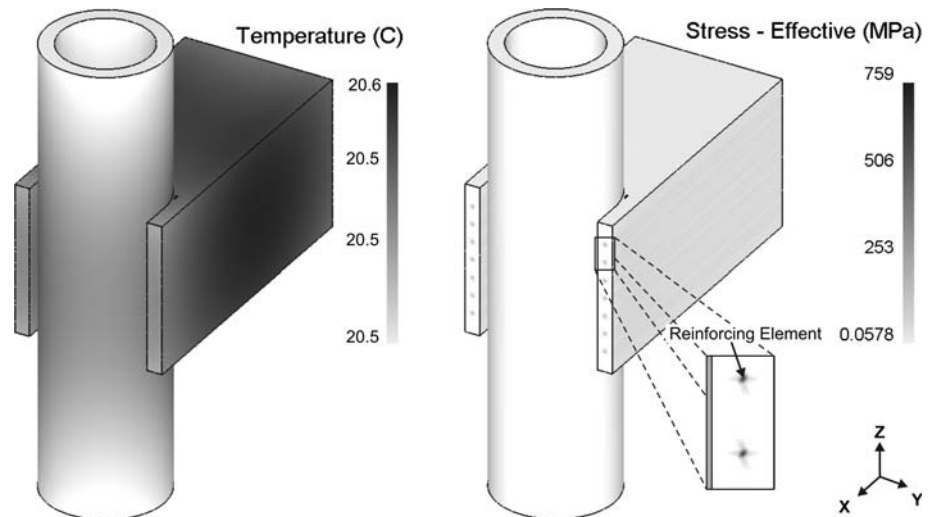
software Deform-3D. A convection coefficient of 0.02 N/ (s mm °C) was used.

The results of the temperature field and the effective stress distribution for the last time step are shown in Fig. 3. It can be seen that very high residual stresses occur, especially in and around the reinforcing elements. The maximum of the effective residual stresses is 759 MPa.

Additionally, in Fig. 4, the stress components are displayed as a result of the numerical calculation. It is obvious that the compressive stresses along the composite profile length are three times higher than those in the other directions. The maximum value here is −946 MPa. Due to the different coefficients of thermal expansion only compressive stresses occur in the reinforcing elements. For steel a coefficient of 1.3e-05 1/K and for aluminium a coefficient of 2.33e-05 1/K were used.

The high residual stress distributions in the reinforcing elements as well as in the aluminium base material can be of great influence for subsequent manufacturing processes. For this reason the node coordinates, the elements and the displayed stress components were exported from Deform-3D in ASCII format to use the residual stresses as initial values for the subsequent manufacturing steps within the process chain.

3 Simulation of the milling process (subproject B2)

3.1 Introduction

In the TR 10 one of the main goals of the simulation projects is to build up a simulation process chain for the simulation of the production of lightweight frame structures. The simulation subproject B3, which integrates the simulation of the milling process, needs the cutting forces as input data for its simulation. These machining forces can either be measured

in a real experiment or can be generated by the simulations of subproject B2. Subproject B2 "Simulation of the five-axis milling process" does not use commercial FEM software, but develops customised simulation methods to meet the demands for a fast milling simulation. In addition to model the progression of material removal, the simulation performs other tasks like the modelling of the tool runout [4], the computation of the occurring machining forces and the resulting dynamic behaviour of the tool [5].

3.2 Overview of the milling simulation

The simulation software of subproject B2 is based on a geometrical/physical model. For the simulation of the dynamic behaviour of the machine tool/tool system, a model of uncoupled harmonic oscillators is used. To calculate the deflection of the tool, all previous forces need to be known. A suitable model for the calculation of the cutting forces is the empiric Kienzle-Victor equation for the oblique cut. Since this formula depends on various geometrical input values of the chip shape, the geometrical conditions of each single cut must be examined in detail. To achieve this, the chip form of each single cut can be constructed by CSG (constructive solid geometry) [6], and its geometric shape can then be measured by calculating intersections between straight lines and the shape of the uncut chip. The tool deflection, which is a result of the forces on the oscillators, is fed back into the next calculation of the chip form. This feedback models the real behaviour, which leads to self-excited chatter for certain machining parameters.

3.3 Construction of the chip form

The milling process can be treated as the removal of the sweep volume of the tool from the work piece. This

444

Prod. Eng. Res. Devel. (2009) 3:441–451

Fig. 4 Stress components after the cooling process from 450 to 20°C
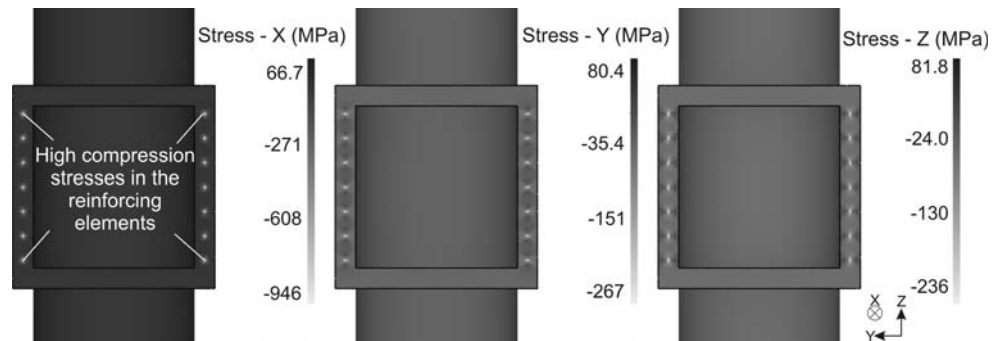
complete process can be modelled by the use of the CSG modelling technique. In CSG a complex solid object is modelled by hierarchically connecting primitive solid objects such as spheres, boxes, cylinders etc. by the Boolean operations union, subtraction, and intersection. The common data structure for a CSG object is a binary tree where the inner nodes stand for the operations and the leafs incorporate the primitives. Boolean operations between volumes can be directly modelled via a CSG tree data structure [6].

The continuous movement of the machine tool is discretised into steps, which can be set to values as small as the movement of a single tooth engagement f_z, whenever a very high simulation quality is needed. Assuming that the NC program consists of linear segments with the length of the tooth engagement f_z, the tool position can be uniquely described by the index of the segment s.

The milling tool is modelled as a union between a cylinder for the shank and, depending on the tool type, a sphere or a torus for the tool tip. A geometrical model of the work piece can be generated by an iterative approach. At the starting time, the work piece W_0 is defined as the starting volume, for example a cuboid (of course, a more complex CSG model is possible). For each new tool position, the tool volume at the corresponding position is subtracted from the work piece. Therefore, the work piece W_s can be described as $W_s = W_0 - \cup_{t=0}^{t \leq s} T_t$ after the cut of the tool at position s where T_t denotes the volume of the tool at position t.

A detailed geometrical description of the tool engagement can also be built up by using CSG. The chip form C_s (Fig. 5) for tool position s, which is fundamental for the calculation of the cutting forces, can be modelled as the intersection between the tool volume at position s and the work piece corresponding to the position of the previous tooth engagement $s - 1$: $C_s = W_{s-1} \cap T_s$.

The size of this chip form can be measured by the calculation of intersections between a straight line and the CSG tree representing C_s.

Since this data structure (and the necessary time for its evaluation) grows with the progression of the simulation,
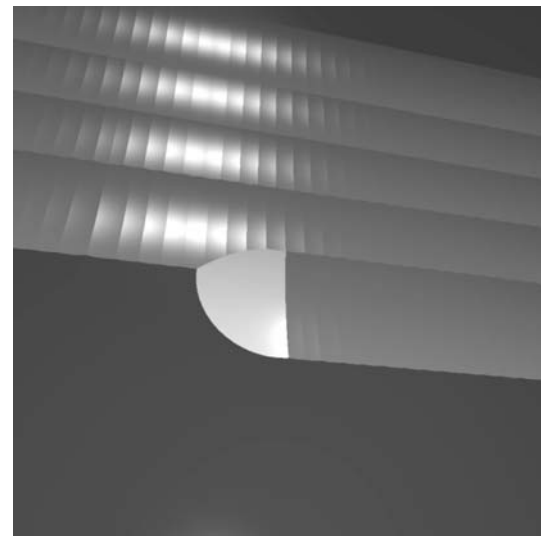
Fig. 5 Surface structure with current chip form (light area)

an enhancement is necessary to achieve simulation times that are feasible in practice. As previous tool engagements, which are far away from C_s, have no influence on its shape, they can be neglected in the calculation. To realise this idea, the NC segments must be added into an octree [7], a spatial data structure, which ensures that NC segments which are near to the current tool position, can be found quickly. After this enhancement, the time consumption for a single examination of a chip shape depends primarily on the complexity of the engagement conditions and no longer on the progression of the simulation.

3.4 Computation of the cutting forces

The calculation of the cutting forces is based on the Kienzle-Victor equation for the oblique cut. For this calculation, the cutting edge is segmented into various cutting wedges. For each wedge, the cutting force in the cutting direction, the force normal to the cutting direction and the tangential force are calculated and added vectorially. The force in cutting direction is calculated by $F_c = b * k_c * h_0 \left(\frac{h}{h_0} \right) 1 - m_c$ where h is the thickness of the undeformed

chip, h_0 is 1 mm, b is the width of the cutting wedge and k_c and m_c are cutting force coefficients. The forces in the other two directions can be calculated accordingly (with different values for the two constants). The sum of the forces on all wedges is the resulting force on the tool.

3.5 Export of the simulation data

The simulation system is a C ++ application for the 32 Bit Microsoft Windows environment. The simulation utilizes the OpenGL application programming interface for the visualisation and interactive manipulation of the view (see Fig. 6).

Typical settings can be loaded from a project file. After a simulation run, the collected simulation data can be saved as comma separated values. Each line of the file contains the simulated distance, the rotation angle of the tool, the respective force on the tool and the dynamic deflection of the tool among other values. To set up a simulation chain, the forces can be imported by subproject B3 using a custom ANSYS script for use in the FEM simulation system.

4 The mechanical FEM simulation of the machining process (subproject B3)

4.1 Introduction

The modelling of machining processes such as the conventional drilling or the circular milling through a macroscopic approach is challenging. Process characteristics like the chip formation, the variable contact conditions between tool and work piece in the contact zone, the heat flux or burr formation have to be considered. Embedding these
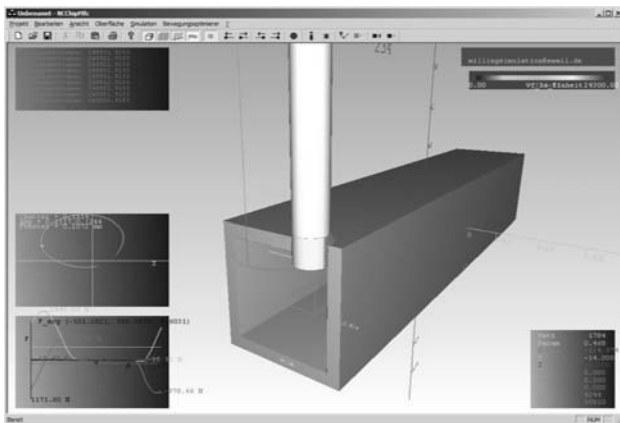
Fig. 6 Screenshot of the running simulation application, in the lower left box the progression of cutting forces is shown, the box above illustrates the trajectory of the tool

aspects into a complete process simulation is very time consuming [8].

Nowadays, simulating machining processes as mentioned above is performed by highly detailed FE-models. These microscopic simulations regard the relative movement between the tool and the work piece, also leading to high computation times [9]. This is caused by the high degree of element deformation in the shearzone which requires a time consuming remeshing of the FE-model between the solving steps. The remeshing process is inevitable due to the increasing deformation of the elements and their negative effects on the solution. The necessary remeshing of the deformed elements is often more time-consuming than the solution of the current load-step. Hence, the microscopic simulation of cutting processes is limited to a small process timeframe. Another disadvantage of the microscopic simulation of cutting processes is the description of the material behaviour through their elastoplastic behaviour. Consequently, the material models are limited in their use because of the unknown strain rates occurring in the shearzone. The required parameters for material models like El-Magd or Johnson–Cook can not be measured with methods like the Split-Hopkinson-Compression-Bar-Test due to the high strain rates [10]. The major influence on the chip formation, beside the heat generation, is contributed by the friction in the primary and secondary shearzone. A global description of the friction law in the contact zone is not constituted so far [8]. In order to reduce the complexity of the macroscopic cutting simulations, an abstract model of the drilling and circular milling was developed at the Institute of Machining Technology (ISF). In contrast to the microscopic simulation, the target values like deformation, stress and (plastic) strain are calculated by applied forces. The relative movement of the tool is substituted for the simulation by the corresponding forces present during the process. Typically, the required data is determined in experiments. In this paper, the feed force and cutting torque moment are simulated by subproject B2. Nevertheless, macroscopic simulations neglect the complex details, mentioned above. So far, this modelling technique is lagging the ability to simulate the chip or burr formation. Here, the main aspect is on the analysis of the work-piece deformation and geometrical deviations [11].

4.2 Idealised modelling of the machining process

For the machining of the component end, a single-tooth milling cutter with a diameter of $d = 12$ mm is used. These specifications were also used in the simulation of the cutting torques performed by subproject B2. The cutting torques are simulated for every single revolution of the

446

Prod. Eng. Res. Devel. (2009) 3:441–451

tool. The maximum value of each revolution is implemented into the ANSYS simulation.

The basis for the presented macroscopic modelling approach consists of the tool substitution, decreasing the modelling effort [12]. The omittance of chip and burr formation is an additional simplification due to the main aim of this research, which is the analysis of the peripheral zone of the hole. As shown in former studies [13], the major and minor cutting edges can be represented by lines, a modelling of the whole tool is not necessary to apply the load onto the workpiece. In this present machining process only the major cutting edge is in contact with the work piece (Fig. 7).

The process is divided into 36 distinct steps to model the continuous stages of the process. Since the machining is simulated for the upper and lower section of the structure, a total of 72 load steps is implemented. The load application is realised by the coupling of a master node with slave nodes in the contact zone. The master node represents the tool centre line for each defined load step. This concept allows the direct joint of the nodes representing the major cutting edge (slave nodes) to the master node. The cutting torque is only applied to the master node and then transferred to the coupled slave nodes. In the current setup, a total of 72 likewise coupled sets is established, each of them representing a different stage of the machining process. After the calculation for one load step, the node coupling and the force loading is deleted from this current master node and changed to the next master node. Since the MSC.Marc source model has been generated without the designated volume to be removed in the arc area, the stepwise removal of the machined material [13] is not integrated.
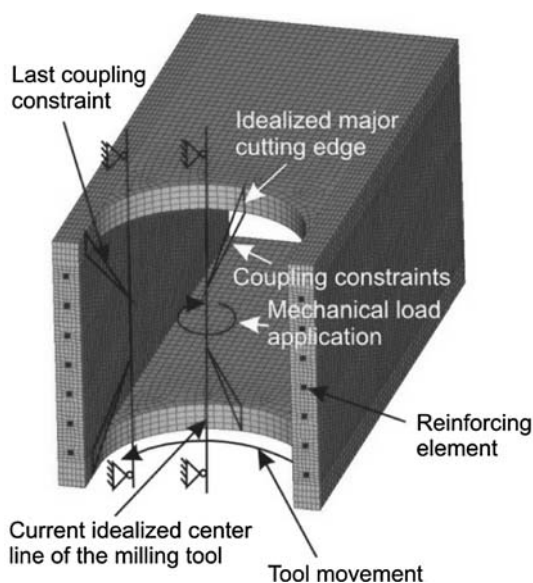

Fig. 7 FE-model of the idealised machining process

4.3 The FE-model considering the process history

As mentioned above, the main goal of the TR 10 is to develop a closed simulation chain, which includes the processes composite extrusion, machining and welding. Therefore, subproject B3 receives process results of the cooling simulation from subproject B1, in particular the residual stresses. Subproject B3 transfers the geometry and stress data from the Deform-3D result file to a readable ANSYS file, in which the machining of the end cross section can be modelled. In the first step the result file of Deform-3D is analysed. The software, which was developed at the ISF, generates several types of files through a Visual Basic script (VBS); where node locations, elements, displacements and residual stresses of the previous Deform-3D simulation are stored. Within the next step, the files are formatted to be read by ANSYS. Therefore, a second script, based on the ANSYS Parametric Design Language (APDL), was developed. It forms nodes and the corresponding elements out of the former Deform-3D result file. In the next programming step, the newly obtained elements are allocated to solid185 8-node-hexaedral elements and an elastoplastic material behaviour is defined (Young's modulus $E = 70,000$ MPa and yield stress $R_{p0,2} = 90$ MPa). The material properties of aluminium EN-AW 6060 are provided by subproject C7. For taking into account the results of the cooling simulation, the nodes are loaded with the residual stresses for realising an initial stress state. The whole structure consists of the reinforced joint and the tube, which is welded subsequently through a laser beam welding process. However, for the simulation of the machining process the tube is not taken into the computation. After the machining simulation the complete structure is transferred to subproject B4, which simulates the laser beam welding of the T-joint. Therefore, another program was developed at the ISF. This programme executes the same operations mentioned above, but in this case the data is converted to a format that can be read by MSC.Marc.

4.4 Results of the mechanical simulation

Figure 8 depicts the equivalent von Mises stresses for the machined workpiece. The von Mises hypothesis is commonly used for ductile materials like steel and aluminium. In contrast to earlier research approaches, the deformation of the work piece is not taken into account within this paper. The cutting parameters for the simulation of the cutting torque moment are set to a cutting speed of $v_c = 400$ m/min and a feed-rate of $f_z = 0.4$ mm. As shown in Fig. 8, the residual stresses after the last load step caused by the machining operation are located around a small zone of the loaded area. Additionally, it is obvious that the

Von Mises
stress

0
11
22
33
44
55
66
77
MPa
100

Maximum stress level
in the contact area
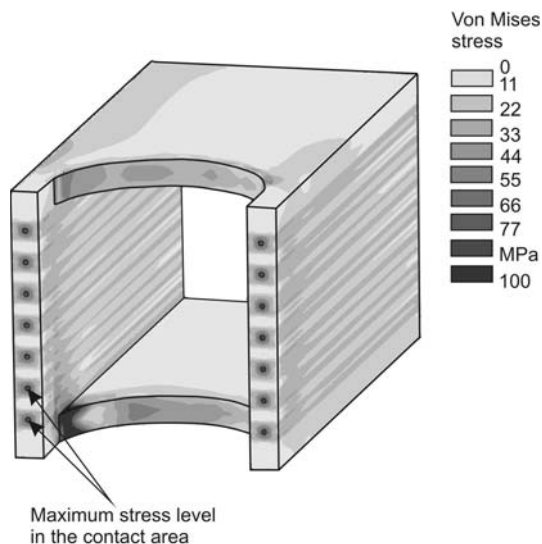
Fig. 8 Resulting von Mises stresses (scaled) after the mechanical simulation

machining of the end zone of the arc geometry is exposed to the highest residual stress. Therefore, the non machined part of the structure is not affected by the machining process itself. With regard to the overall stress distribution, it can be seen that the machining process itself has lower impact on the overall structure, in comparison to the cooling of the extruded profile.

As mentioned above, the stresses of the cooling simulation have to be transferred to the ANSYS database. Since the mechanical simulation is only affecting the non-reinforced parts of the profile, the residual stresses in the contact area between the steel elements and the aluminium matrix are presumably not altered. The computed residual stresses for a representative reinforcing element are also illustrated in Fig. 8. It can be seen that the stresses in the contact area are significantly higher than those in the rest of the surrounding aluminium matrix. For illustrating purposes, the result plot has been scaled to a maximum of 100 MPa. Hence, the overall stress level of the ANSYS simulation is in a good accordance with the Deform-3D simulation performed by subproject B1. It has to be mentioned that the used mesh is relatively coarse for a mechanical simulation. A refinement of the mesh, especially in the loaded area, is suited to compute even more accurate results.

5 Simulation of the welding process (subproject B4)

5.1 Introduction

The examined process chain ends with a welding process. In detail, two laser beam welds are executed to join the tube and the square profile together. These welds are indicated in Fig. 9.

The feed for the laser beam is set to 33 mm/s. The second weld starts directly after the first weld. For both welds a pitch of 45° is applied. During the welding operations the tube is clamped rigidly while the square profile is held in place. Due to the positioning of the welds there is no direct interaction between the laser beam and the reinforcing elements. Thus, the welding process remains stable.

5.2 Simulation fundamentals and data import

The investigated laser beam welding process is examined by means of a structural welding simulation, which is based on the finite element method [14]. The commercial software tool MSC.Marc Mentat was used for this simulation. A heat source is applied to simulate the heat input into the part [15]. Additionally, several boundary conditions have to be set. The clamping conditions were realised as rigid constraints and the heat transfer to the surroundings was defined to happen by convection and radiation. The coupled thermo-mechanical simulation is divided into two steps according to the real welding process. Firstly, the clamped part is welded and cools down to ambient temperature while still being clamped. Afterwards, the clamps are removed and the part reaches its final state.

As before, the final state of the previous step has to be set as the initial state of the current simulation to realise an integrated process chain. The result data provided by subproject B3 was used to define the respective initial state. This was realised by converting the results to the appropriate format and by then saving the data in a MSC.Marc result file which was used to restart the welding simulation. Thus, the welding simulation starts with high residual stresses in the reinforcing elements. Due to the different positions of the reinforcing elements relative to the welding zones some reinforcements are more influenced by the heat input than others. Overall the welding process has a significant effect on the stress state of the composite material. As for the composite extrusion process the change in the residual stress state is mainly caused by the different material properties of aluminium and steel.

5.3 Results of the simulation

The most important results of the simulations are the temperature field, the structural distortions and the residual stresses. The following figures represent a selection of the computed results. On the left side Fig. 9 shows the temperature field during the first welding operation. The molten material is clearly visible as a dark area.

Figure 9 illustrates on the right side the residual stresses after the welding operation is finished. At the same time

448

Prod. Eng. Res. Devel. (2009) 3:441–451

Fig. 9 Temperature field during the first weld (*left*) and residual stresses of the T-joint in its final state (*right*)
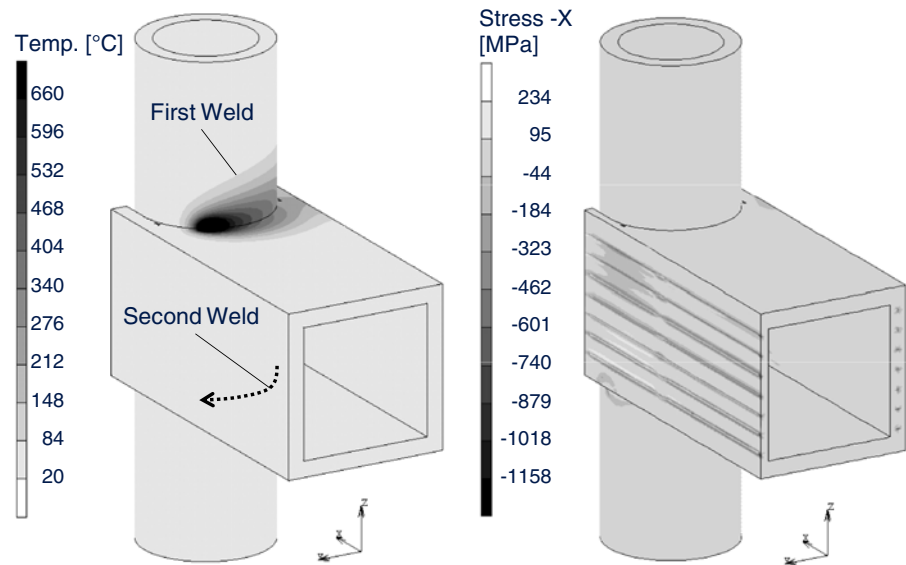
this is the final state of the whole process chain. To visualise the stress state in the reinforcing elements half of the left wall of the square profile was masked. These results are discussed more detailed in chapter 7.

6 Realisation of the virtual process chain using a single universal FE-software (subproject C7)

6.1 Introduction

To make valid predictions about the final state of a product at the end of a process chain it is necessary to consider the manufacturing history regarding the structural properties of the work piece. In general, specific software tools are used to analyse the various manufacturing processes. Problems arise when trying to couple the different software systems for an integrated simulation chain. These problems are mainly caused by unequal data formats. Thus, software interfaces are required as exemplarily shown in the previous chapters.

To avoid the interface problems this chapter introduces an alternative approach for the simulation of a process chain. Here, the universal FE-software MSC.Marc Mentat is used to realise the virtual process chain with only a single program. However, this method requires certain knowledge of the included manufacturing processes or rather the structural effects of these processes on the work piece. The general idea is to identify the significant structural influences of the different processes with regard to the entire process chain. This means, that not every process effect or complete process step respectively has a relevant effect and may be disregarded. The implementation of this

approach is discussed in the next section for the exemplary part.

6.2 Simulation fundamentals

Firstly, the interesting physical values of the examined part have to be identified. In this work structural distortions and residual stresses are the most important values with respect to the product quality. Concerning these structural properties, the composite extrusion process can be mainly characterised by a cooling phase from 450°C to ambient temperature. As mentioned above, this is because of the different thermal expansion coefficients of the involved materials. Thus, the complete first process step can be modelled by setting the initial temperature to 450°C and by defining a simple boundary condition. The latter describes the time-dependent coefficients of radiation, convection and conduction.

As shown in [16] and [17], the residual stresses induced by machining are limited in a region with a maximum depth of 0.15–0.2 mm. Thus, the structural effects are restricted locally, provided that no reinforcing element is embedded in the machined zone. Furthermore, the magnitude of these effects is small and negligible if heat dominated manufacturing processes are involved [18]. Additionally, these assumptions are corroborated by the results of the simulation of the milling process shown above. Therefore, the milling process was neglected for this approach.

Finally, the welding operations had to be modelled. Due to the fact that the same software tool was used as for the first approach the already defined settings could be adapted. Thus, the description given above applies for this case as well.

6.3 Results of the simulation

In the following figure (Fig. 10) the residual stress state at the end of the whole process chain is shown. As in Fig. 9, half of the left wall of the square profile is not displayed to better visualise the stresses in the reinforcing elements.

7 Analysis and comparison of the computed results

The first approach that was investigated clearly reveals the significance of considering the process history for making statements about the final product quality. The composite extrusion that was represented by a cooling phase does generate high compressive stresses in the reinforcing elements. Their formation is mainly caused by the different coefficients of thermal expansion of steel and aluminium respectively. The milling operation induces local stresses whose magnitude is minor in comparison to the other manufacturing operations. Finally, the welding process that is separated into two welding steps influences the residual stress state significantly. As seen in Fig. 10, the compressive stresses in the reinforcing elements increase even more due to the process. These findings are supported thoroughly by the results of the second approach. To compare the
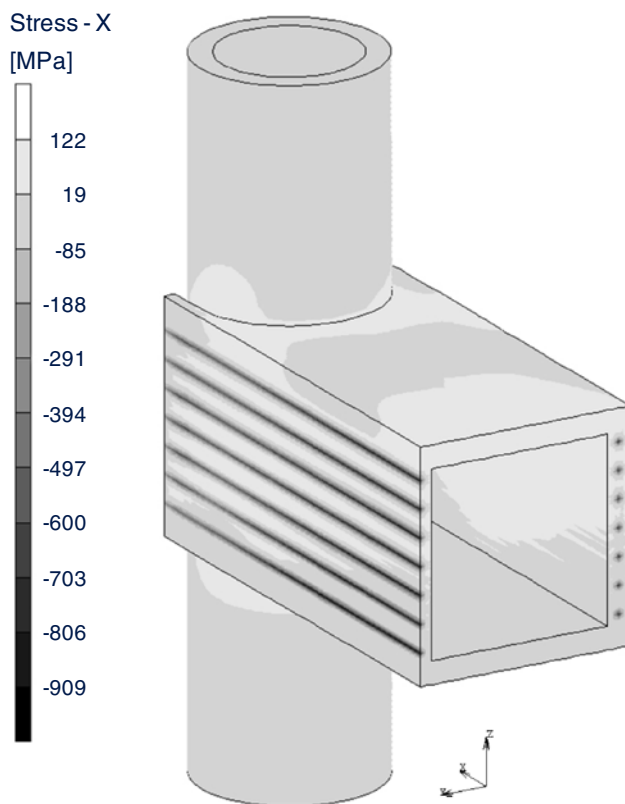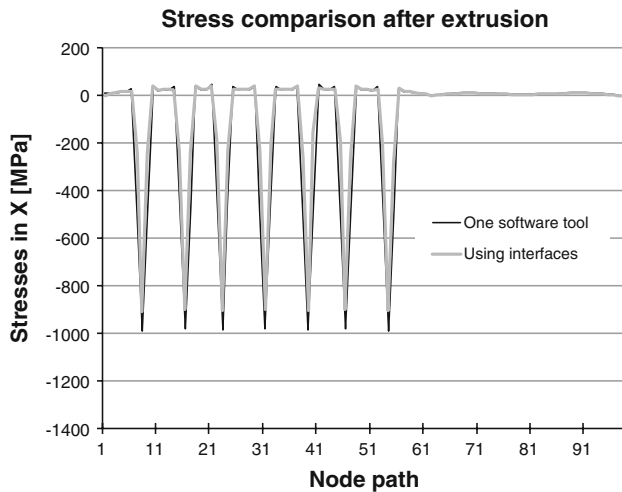
results of both methods a node path is specified through the square profile as pictured in Fig. 11. For the comparisons in Figs. 12 and 13 the stress value in x-direction at every node (1–97) along the node path is taken into account. Hereby, the node path is chosen in such a way that the potential effects of every process in the process chain are represented.

Figure 12 shows a comparison of the stress states after the extrusion process and before the milling operation for both methods. The results of both methods are in high accordance. The compressive stress peaks in the reinforcing elements are clearly visible as well as their equal magnitude for each particular method. The latter is due to the solely volumetric change of the part during the cooling and thus the deviatoric component of the strain tensor is zero. The high compressive stress level in the reinforcing elements is in good accordance with measurements done by means of neutron diffraction. This experimental investigation was performed by a collaboration of several subprojects of the TR 10 and will be published soon.

Continuing the above examinations, Fig. 13 compares the stress state for the welding processes for both methods after the T-joint is cooled down to ambient temperature. For the approach using interfaces these results include the effects of the milling process. Hereby, the direct influence of the process affects a section of the work piece, which is represented by the nodes 63–97. However, the influence is marginal when comparing the curves in this interval of nodes and keeping in mind that the black curve does not consider the milling process at all. Contrary to the cutting process the welding operation has a significant influence in the directly affected section as well as in the rest of the work piece and can not be neglected. As Fig. 13 shows,

Fig. 10 Residual stresses of the T-joint at the end of the process chain
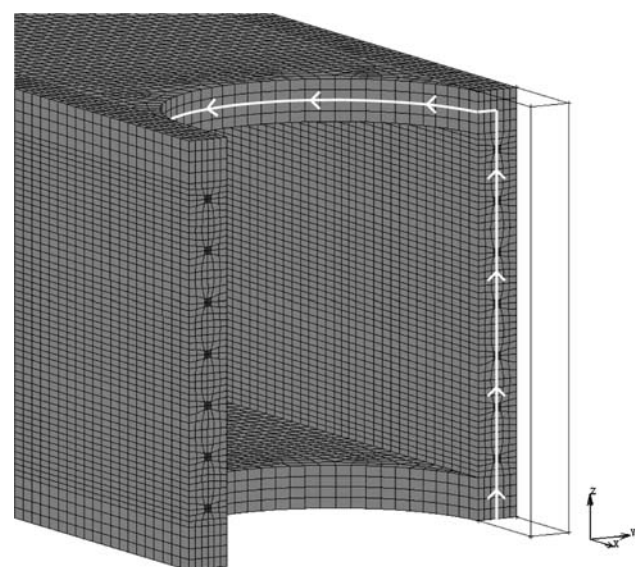
Fig. 11 Node path for the stress comparison of both methods

450

Prod. Eng. Res. Devel. (2009) 3:441–451

Stress comparison after extrusion

Fig. 12 Stress comparison for both methods along the specified node path (Fig. 11) after the extrusion process (cooling process)

Stress comparison at the final state
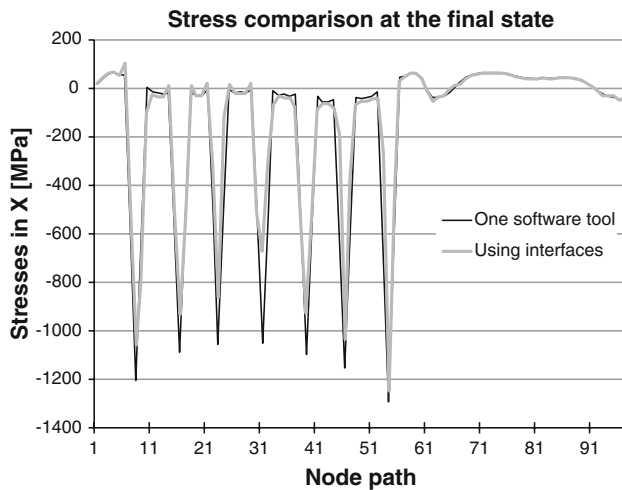
Fig. 13 Stress comparison for both methods along the specified node path (Fig. 11) at the end of the process chain

also the compressive stresses in the reinforcing elements increase. Hereby, the effect on the reinforcing elements depends on their position relative to the welding zone as the different peaks in Fig. 13 indicate.

Generally, a good consistence between both curves can be stated. The differences in the peak values will be further investigated.

When comparing both approaches different aspects have to be taken into account. In principle, the chaining of various program to a virtual process chain provides more exact results than the shown alternative, but makes interfaces necessary to exchange the result data. A single universal software system eliminates the need of interfaces, but requires certain modelling simplifications to simulate the whole process chain. On the other hand, technological know-how of the involved processes is needed. The

comparison of the residual stresses shows a good consistency of both approaches. Thus, the second approach did show the potential to predict the final quality of the product and hence the possibility to improve it.

8 Conclusions

In the work presented here an integrated virtual process chain was realised for the processes composite extrusion, milling and welding. Thus, the effect of every manufacturing step along the process chain can be incorporated in the simulation and contributes to the part's final state. Furthermore, it is possible to analyse the individual processes and to quantify their overall influence on the final results. Although the simulation methods were applied to a single exemplary part, they can be adapted to other geometries without restrictions. The comparison of the two approaches shows that both methods are capable to realise a virtual process chain that includes the influences of the process history.

References

1. Schomäcker M (2007) Verbundstrangpressen von Aluminiumprofilen mit endlosen metallischen Verstärkungselementen. Dissertation, Institute of Forming Technology and Lightweight Construction. Shaker, Dortmund, ISBN 978-3-8322-6039-2
2. Schikorra M, Schomäcker M, Kloppenborg T, Tekkaya AE, Weidenmann K, Kerscher E, Löhe D (2007) Improved properties of aircraft stringer profiles by composite extrusion. In: Proceedings of the international conference on applied production technology (APT-07), Bremen (Germany), 17–19 September 2007, Conference Proceedings, pp 285–292, ISBN 978-3-933762-21-4
3. Schikorra M (2006) Modellierung und simulationsgestützte Analyse des Verbundstrangpressens. Dissertation, Universität Dortmund. Shaker, Dortmund, ISBN 3-8322-5506-0
4. Weinert K, Surmann T, Enk D, Webber O (2007) The effect of runout on the milling tool vibration and surface quality. In: Production engineering 1:3. Springer, Berlin/Heidelberg, ISSN 0944-6524 (Print) 1863–7353 (Online). doi:10.1007/s11740-007-0053-5, S. 265–270
5. Weinert K, Surmann T (2006) Modeling of surface structures resulting from vibrating milling tools. Production engineering—research and development, Annals of the German Academic Society for Production Engineering, XIII, 2, pp 133–138
6. Foley JD, Van Dam A, Feiner SK, Hughes JF (1995) Computer graphics: principles and practice in C, ISBN 0201848406
7. Abramowski S, Müler H (1991) Geometrisches Modellieren, Bibliographisches Institut & F.A. Brockhaus AG, Mannheim, Germany, ISBN 3-411-14491-2
8. Soehner J (2003) Beitrag zur Simulation zerspanungstechnologischer Vorgänge mit Hilfe der Finite-Elemente-Methode. Dissertation, Universität Karlsruhe (TH), Germany

9. Oh J-D (2004) Modellierung und Simulation des mechanischen und thermischen Beanspruchungsverhaltens metallischer Werkstoffe bei der Spanbildung. Dissertation, Technische Universität Kaiserslautern, Germany
10. Piendl S, Aurich JC, Steinicke M (2005) 3D finite-element simulation of chip formation in turning. Proceedings of the 8th CIRP international workshop on modelling of machining operations, Chemnitz, Germany, pp 225–234
11. Weinert K, Biermann D, Kersting M, Grünert S (2008) Experimental and computational analysis of machining processes for light-weight aluminium structures. TTP Trans Tech Publications Ltd, Switzerland, Advanced Materials Research vol 43, pp 97–104
12. Weinert K, Grünert S, Hammer N, Kersting M (2005) Analysis of circular milling processes for thin-walled space-frame-structures applying FEA-simulation. Production engineering-research and development, Annals of the German Academic Society for Production Engineering, XII, 1, pp 99–102, ISBN 3-9807670-6-x
13. Weinert K, Grünert S, Kersting M (2006) Analysis of cutting technologies for lightweight frame components. In: Kleiner M et al (ed) Flexible manufacture of lightweight frame structures, TTP Trans Tech Publications Ltd., Switzerland, vol 10 of Advanced Materials Research, pp 121–136, ISBN 0-87849-403-0
14. Radaj D (1992) Heat effects of welding—temperature field, residual stresses, distortion. Springer, Berlin
15. Goldak JA, Akhlaghi M (2005) Computational welding mechanics. Springer, New York
16. Jacobus K, Kapoor SG, DeVor RE (2001) Experimentation on the residual stresses generated by endmilling. J Manuf Sci Eng 123:748–753
17. Jacobus K, DeVor RE, Kapoor SG (2000) Machining-induced residual stress: experimentation and modeling. J Manuf Sci Eng 122:20–31
18. Dattoma V, De Giorgi M, Nobile R (2006) On the evolution of welding residual stress after milling and cutting machining. Comput Struct 84:1965–1976